# Electron-spin-resonance studies of the ferrimagnetic semiconductor FeCr2S4

**Vladimir Tsurkan, Meike Lohmann, Hans-Albrecht Krug von Nidda, Alois Loidl, Siegfried R. Horn, Reinhard Tidecks**

**Angaben zur Veröffentlichung / Publication details:**

Tsurkan, Vladimir, Meike Lohmann, Hans-Albrecht Krug von Nidda, Alois Loidl, Siegfried R. Horn, and Reinhard Tidecks. 2001. "Electron-spin-resonance studies of the ferrimagnetic semiconductor FeCr2S4." *Physical Review B* 63 (12): 125209. https://doi.org/10.1103/PhysRevB.63.125209.



# Electron-spin-resonance studies of the ferrimagnetic semiconductor $FeCr_2S_4$

V. Tsurkan,[1,2] M. Lohmann,[1] H.-A. Krug von Nidda,[1] A. Loidl,[1] S. Horn,[1] and R. Tidecks[1]
[1]*Institut für Physik, Universität Augsburg, Universitätsstraße 1, D-86159 Augsburg, Germany*
[2]*Institute of Applied Physics, Academy of Sciences of Moldova, Academiei 5, MD 2028, Chisinau, Republic of Moldova*
(Received 18 October 2000; published 13 March 2001)

Electron-spin-resonance (ESR) measurements have been performed on $FeCr_2S_4$ single crystals in the temperature range 4.2–200 K. On decreasing temperature, the resonance lines strongly shift to low fields for the easy magnetization direction, ⟨100⟩, and to high fields for the hard directions, ⟨110⟩ and ⟨111⟩. In the hard directions additional resonance modes appear below 125 K. The nonmonotonic behaviors of the ESR linewidth and intensity indicate substantial changes of the relaxation processes below 125 K, which correlates with the macroscopic dc magnetization and ac susceptibility data.

DOI: 10.1103/PhysRevB.63.125209 PACS number(s): 75.50.Pp, 76.50.+g, 75.30.Gw

## I. INTRODUCTION

The ternary $FeCr_2S_4$ ferrimagnetic semiconductor shows correlated transport and magnetic properties. The observation of a colossal magnetoresistance similar to that of manganese perovskites,[1] and of a half-metallic behavior,[2] has attracted considerable interest in this material. It has a normal spinel structure with two magnetic sublattices occupied by tetrahedrally coordinated Fe and octahedrally coordinated Cr ions which order antiferromagnetically below the Curie temperature $T_C$ (~170 K).[3] High-field magnetization measurements indicate a strong magnetocrystalline anisotropy due to the presence of $Fe^{2+}$ ions tetrahedrally surrounded by sulphur ions.[4,5] Recently, the unusual behavior of the low-field dc magnetization of $FeCr_2S_4$ single crystals, similar to that of a spin glass, was observed below 60 K.[6,7] ac susceptibility measurements revealed considerable temperature-dependent magnetic relaxation processes at low temperature.[8] The origin of these phenomena is not clear at present. Structural changes may be the reason. Electron-spin resonance (ESR) is a powerful technique for the investigation of spin-lattice and spin-spin relaxation phenomena in magnetic materials, and is thus suitable to improve the knowledge about the dynamic magnetic properties of this compound. As far as we know, this is the first ESR study on $FeCr_2S_4$ single crystals.

## II. EXPERIMENTAL TECHNIQUES

$FeCr_2S_4$ single crystals were grown by the chemical transport reaction method,[9] with chlorine as the transport agent. The sample composition was checked by energy-dispersive x-ray analysis. The single-phase spinel structure of the samples was confirmed by x-ray-diffraction analysis. ESR measurements were performed for $4.2\,\mathrm{K} < T < 200\,\mathrm{K}$, using a Bruker ELEXSYS E500 cw $X$-band spectrometer with frequency modulation of the magnetic field, and recording the field derivative of absorption, $dP/dH$, with a lock-in technique. Samples were mounted in a continuous He gas-flow cryostat (Oxford Instruments), and the temperature stability was about 0.3 K. Measurements were performed on polished thin disks with (001), (110), and (111) plane orientations for parallel and perpendicular configurations of the magnetic field to the plane surface. Perfect octahedron-shaped as-grown single crystals and polycrystalline samples were also studied. The orientation of the single crystalline samples in the principal directions was better than ~2°. In all measurements the frequency was $\upsilon = 9.478\,\mathrm{GHz}$.

## III. EXPERIMENTAL RESULTS

Figure 1(a) presents typical ESR spectra at a selected temperature below $T_C$ for one of the disklike samples with a (110) plane orientation, recorded in the parallel configuration

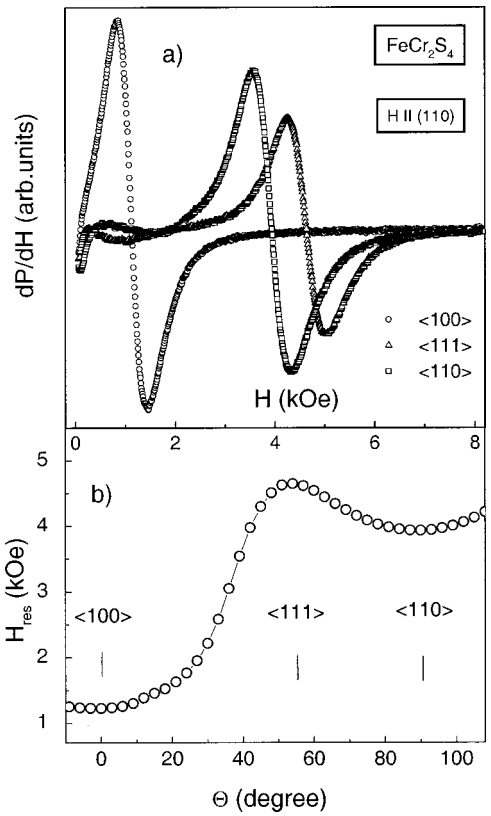


FIG. 1. (a) ESR spectra of a $FeCr_2S_4$ single crystal (sample Fe 35$m$, disk) at 105 K for the $H\|(110)$ plane along three principal axes. (b) Angular dependence of the resonance field for the same sample at 105 K.

 

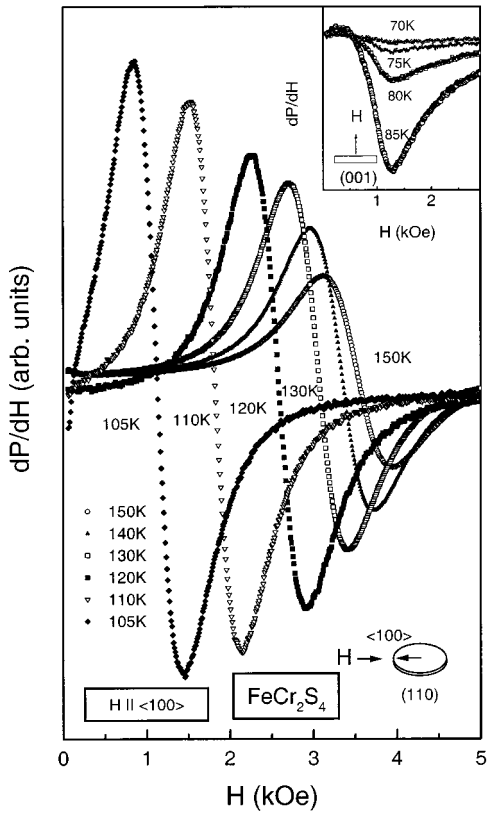


FIG. 2. ESR spectra of a $FeCr_2S_4$ single crystal (sample Fe $35m$, disk) at different temperatures for the $H\|(110)$ plane. $H$ is applied in the easy magnetization direction $\langle 100\rangle$. Inset: ESR spectra for perpendicular orientation [sample Fe $35e$, disk, plane $(100), H\|\langle 001\rangle$].

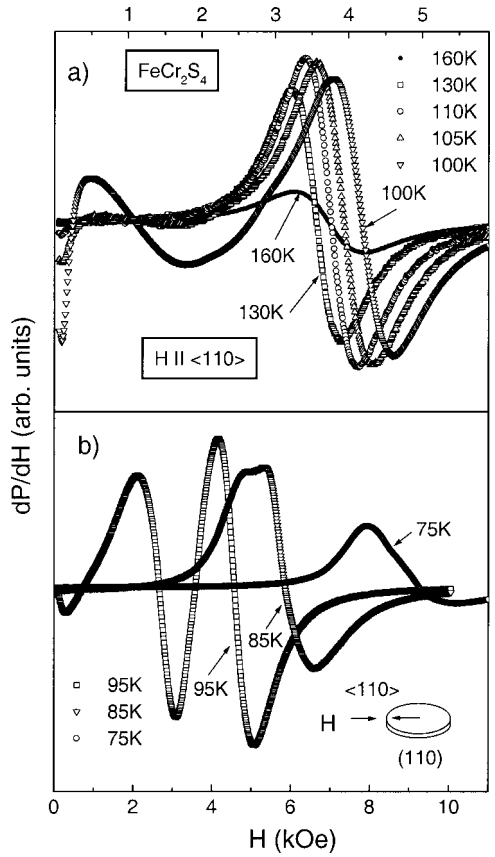


FIG. 3. ESR spectra of a $FeCr_2S_4$ single crystal (sample Fe $35m$, disk) at different temperatures for $H\|\langle 110\rangle$.

with the magnetic field $H$ along the three main crystallographic directions, $\langle 100\rangle$, $\langle 111\rangle$, and $\langle 110\rangle$. The spectra are strongly angle dependent, as shown in of Fig. 1(b), with different temperature behaviors for different axes. Figure 2 shows the field dependence of the ESR signal at various temperatures for the same sample, with the magnetic field along the easy magnetization direction $\langle 100\rangle$. In the paramagnetic state above 167 K no ESR signal was found. Decreasing the temperature from 165 to 105 K yields an increase of the ESR line intensity and a shift of the resonance to lower fields. For further decreasing temperatures the intensity of the ESR line significantly decreases. A similar behavior of the resonance line for $H$ in the $\langle 100\rangle$ direction was observed for the (001) plane both for parallel and perpendicular configurations. In the inset of Fig. 2, ESR spectra for temperatures between 90 and 60 K are presented. Below 60 K no ESR resonance line could be detected in the $\langle 100\rangle$ direction.

The ESR spectra for $H\|\langle 110\rangle$ axis exhibit a completely different behavior than for $H\|\langle 100\rangle$ (see Fig. 3). On decreasing temperature, $160\,\mathrm{K} < T < 135\,\mathrm{K}$, the resonance lines are shifted to lower fields, whereas for temperatures below 130 K they are shifted to higher resonance fields. At temperatures below 125 K, a second resonance line is observed in the low-field region. The second resonance line is shifted to higher fields with decreasing temperature, like the main line. Below 90 K these two lines merge and continuously shift to higher fields, with an increasing rate for decreasing temperature.

In the $\langle 111\rangle$ direction the ESR spectra show a similar temperature behavior as for the the $\langle 110\rangle$ axis. The rate of the temperature shift of $H_{\mathrm{res}}$ is considerably higher than for the $\langle 110\rangle$ direction in the range 140–80 K. Below 70 K the resonance field in the $\langle 111\rangle$ direction becomes smaller than that in the $\langle 110\rangle$ direction. At temperatures below 60 K, ESR lines in the hard directions become strongly distorted.

In the temperature range $90\,\mathrm{K} < T < 160\,\mathrm{K}$ the main ESR line was found to have a pure Lorentzian shape, and from the corresponding fit of the spectra the values of the resonance field, $H_{\mathrm{res}}$ of the linewidth, $\Delta H$, and of the integral intensity, $I$, were calculated. Figure 4 shows the temperature dependences of these parameters for the three directions investigated for a disk of (110) plane in parallel configuration. The linewidth $\Delta H$ in the $\langle 110\rangle$ and $\langle 111\rangle$ directions exhibits a nonmonotonic temperature change with a minimum at around 125 K, whereas in the $\langle 100\rangle$ direction $\Delta H$ decreases continuously with decreasing temperature [Fig. 4(b)]. A nonmonotonic behavior of the integral intensity of the ESR signal is a characteristic feature of all three directions [Fig. 4(c)]. Similar variations of the ESR spectra were observed for (100) and (111) planes in parallel and perpendicular configurations. However, below 90 K the data on $I$ and $\Delta H$ should be treated with caution because of the strong distortion of the ESR lines.

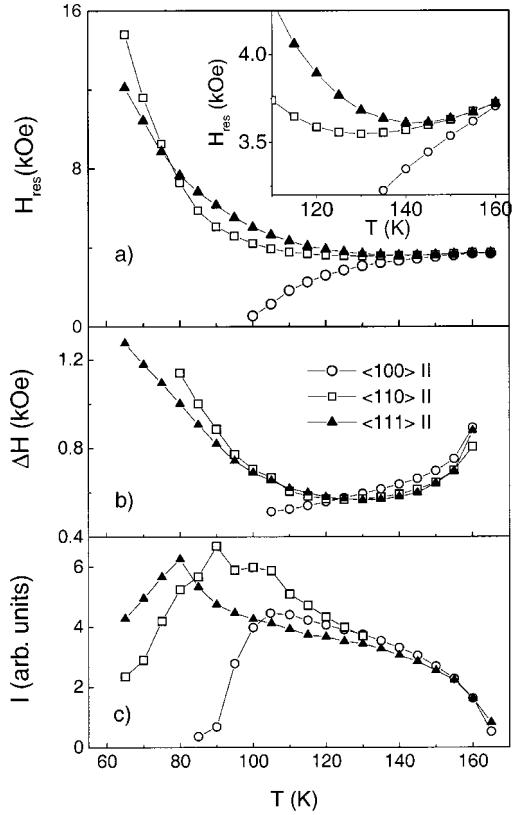


FIG. 4. Temperature dependences of the resonance field $H_{res}$ (a), linewidth $\Delta H$ (b), and integral intensity I (c), of a $FeCr_2S_4$ single crystal (sample Fe 35$m$, disk) for three principal crystal axes. Inset: $H_{res}=f(T)$ for the same sample at increased scales at high temperatures.

## IV. DISCUSSION

The evolution of the resonance fields with decreasing temperature in the range 160–60 K can be understood in terms of a ferromagnet with a strong cubic anisotropy. The resonance conditions in a ferromagnetic sphere for the magnetic field applied in the three main directions ⟨100⟩, ⟨110⟩, and ⟨111⟩ are given by the relations[10]

$$\langle 100\rangle: \quad \omega/\gamma = H_{res} + 2H_A, \tag{1}$$

$$\langle 111\rangle: \quad \omega/\gamma = H_{res} - 4H_A/3, \tag{2}$$

$$\langle 110\rangle: \quad \omega/\gamma = \{(H_{res} - 2H_A)(H_{res} + H_A)\}^{1/2}, \tag{3}$$

where $\omega$ is the resonance frequency, $\gamma$ is the gyromagnetic ratio ($\gamma = ge/2mc$), $g$ is the spectroscopic splitting factor, $H_A = K_1/M$ is the anisotropy field, $M$ is the sample magnetization, $K_1$ is the first-order anisotropy constant, and the second-order anisotropy constant is neglected.

Using Eqs. (1)–(3) we calculated the field dependence of the resonance frequencies. In Fig. 5 these theoretical curves are plotted, normalized to the anisotropy field $H_A$. According to Eqs. (1)–(3) an anisotropy field $H_A$ for fixed $\omega$ shifts the resonance field in the ⟨100⟩ direction to low fields, whereas for the ⟨111⟩ and ⟨110⟩ directions this shift is in the opposite direction. In the ⟨110⟩ direction for large values of

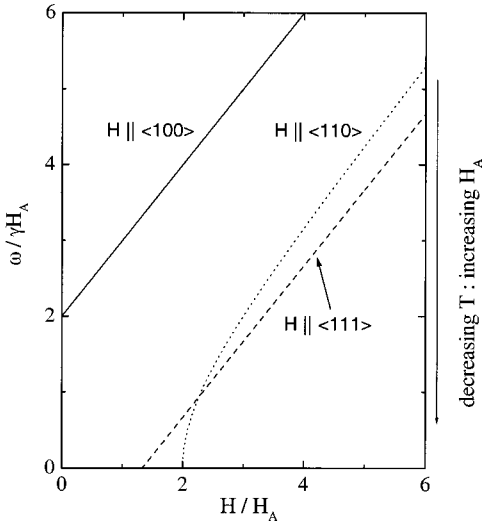


FIG. 5. Dependence of the resonance frequency $\omega/\gamma$, normalized to the anisotropy field $H_A$, on an applied magnetic field $H$ normalized to $H_A$.

$\omega/\gamma H_A$, i.e., low values of the anisotropy field, the resonance field $H_{res}$ is smaller than in the ⟨111⟩ direction, but for higher $H_A$ the situation is reversed, as can be seen from Fig. 5. In our experiment $\omega$ is fixed, but $H_A$ varies with temperature. The anisotropy field $H_A$ increases with decreasing temperature,[5] so that $\omega/\gamma H_A$ decreases with decreasing temperature. Thus Fig. 5 explains very well the experimentally observed behavior of the resonance field with temperature for all three directions studied [Figs. 4(a) and 6(a)].

The values of the anisotropy field plotted in Fig. 6 were calculated from Eqs. (1) and (2) using the measured values of resonance field $H_{res}$ for these two directions, and considering that $\omega/\gamma$ is constant. We now justify the use of the above-mentioned formulas to calculate the anisotropy field for our nonspherical samples, in which a shape anisotropy may play a role. As is well known,[11] only in the case of a sphere is no shift of the resonance field by demagnetizing fields expected, because the demagnetizing contributions along the main axes cancel each other. For our octahedron sample in all three principal directions the resonance field $H_{res}$ is not changed in the temperature range above 150 K [see the inset of Fig. 6(a)]. This indicates a small contribution of the anisotropy field, which is temperature dependent and could yield a temperature dependence of $H_{res}$. Moreover, for these temperatures the experimental values of the resonance field are the same for the ⟨111⟩ and ⟨100⟩ axes. The value of $H_{res}$ in the ⟨110⟩ direction for this temperature range is only slightly lower (by ~1%) than for the ⟨111⟩ and ⟨100⟩ directions. Thus the demagnetizing fields, which could lead to some angular dependence due to differences in shape, or to a temperature dependence due to the temperature dependence of the magnetization, are negligible. For this reason we consider the octahedron sample as a sphere and use Eqs. (1)–(3) for the calculation of the anisotropy field.

For the disklike sample (see the inset of Fig. 4) at high temperatures between 150 and 160 K, where the contribution of the anisotropy field is small, the demagnetizing field shifts

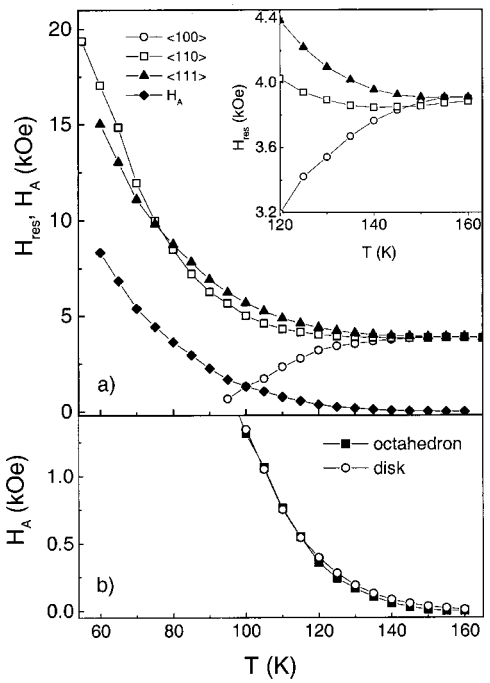


FIG. 6. (a) Temperature dependences of the resonance field $H_{\mathrm{res}}$ for three principal crystal axes and of the anisotropy field $H_A$ of a $FeCr_2S_4$ single crystal (sample Fe 35*u*, octahedron). Inset: $H_{\mathrm{res}}=f(T)$ for the same sample at increased scale at high temperatures. (b) Temperature dependences of the anisotropy field $H_A$ for samples Fe 35*m* and Fe 35*u*.

the resonance for all three directions to lower fields, as one expects from the Kittel formula for ferromagnetic resonance in an in-plane magnetized disk.[11,12]

The temperature dependence of the anisotropy field obtained experimentally from the resonance fields for the octahedron sample is shown in Fig. 6, together with data obtained for the disklike specimen which is magnetized within its plane. The calculated values of the anisotropy field $H_A$ in both cases are close, indicating that contribution of the shape anisotropy is small. For temperatures where the resonance field in $\langle 100\rangle$ direction is clearly determined, we calculated $H_A$ from the difference of the resonance fields in $\langle 111\rangle$ and $\langle 100\rangle$ directions, as explained above. From the resulting values of $H_A$ using Eqs. (1) or (2), we calculated $\omega/\gamma$ as the function of temperature for the range 160–100 K. This yields a value of $\omega/\gamma\sim 3900$ Oe, independent of temperature within $\sim$2%. For lower temperatures ($T<100$ K), where the resonance field in the $\langle 100\rangle$ direction cannot be evaluated, we used the resonance field for the $\langle 111\rangle$ direction together with the $\omega/\gamma$ value mentioned above, which is assumed to be also constant below 100 K. This assumption is justified using Eqs. (2) and (3), though only within $\pm 10\%$, according to an increase of the error in the determination of $H_{\mathrm{res}}$ caused by complicated shape of the resonance curve. The values of the anisotropy field calculated in this way are in agreement with the data obtained from the high-field magnetization measurements on the same single crystals (which will be published elsewhere).

The experimentally found value of the resonance field, $\sim$3900 Oe for the octahedron sample at high temperatures, where the contribution of the anisotropy field is low [see the inset of Fig. 6(a)] strongly deviates from the value 3386 Oe calculated for $g=2$ according to the formula[12]

$$h\nu = g\mu_B H_{\mathrm{res}}, \tag{4}$$

where $\mu_B$ is the Bohr magneton. This can be understood taking by into account the presence of two antiparallel aligned magnetic sublattices. For ferrimagnetic substances, like ours, the effective $g$ factor is given by the formula[10,13]

$$g_{\mathrm{eff}} = (M_1 - M_2)/(M_1/g_1 - M_2/g_2), \tag{5}$$

where $M_1, M_2$ and $g_1, g_2$ are magnetic moments and $g$ factors of the two sublattices, respectively. Using the single-ion value for Fe and Cr moments and $g$ values of these ions in similar substances,[14,15] one can easily obtain the observed value of the resonance field. For example, for $g_{\mathrm{Fe}}=2.07$ and $g_{\mathrm{Cr}}=1.95$, the calculated value of the resonance field is 3876 Oe, which is close to the observed one.

The appearance of additional low-field resonance lines in the hard magnetization directions $\langle 110\rangle$ and $\langle 111\rangle$ may result from the nonsaturated state. Indeed, the field position of these additional lines corresponds to an incomplete alignment of the magnetization vector by the applied field.[7] Similar additional low-field resonance lines were often found in nonsaturated multisublattices ferrimagnets (see, for example, Ref. 16).

The nonmonotonic temperature behavior of the linewidth of the ESR signal [Fig. 4(b)] reflects the contribution of different mechanisms. One of these, probably caused by critical fluctuations, determines the decrease of $\Delta H$ around the magnetic phase transition. The increase of the resonance linewidth at temperatures below 125 K may be related to some inhomogeneous broadening due to lattice distortions induced, for example, by the Jahn-Teller effect or by magnetostriction. These effects were envoked for explanation of the Mössbauer spectra anomalies of $FeCr_2S_4$.[17–21] The appearance of lattice distortions in $FeCr_2S_4$, and their increase with decreasing temperature, were found earlier as a broadening of x-ray-diffraction lines at temperatures below $T_C$.[22] If this mechanism is of significance here, then our ESR data give evidence of a strong spin-lattice coupling in this compound.

Since our samples have a relatively low resistivity, we should discuss a possible influence of the skin effect on our results. We estimated the penetration depth $\delta$ by the formula[23]

$$\delta = (\rho/\mu_0\omega)^{1/2}. \tag{6}$$

There is a minimum of the resistivity $\rho$ observed at around 125 K with the value $\rho = 4.5\times 10^{-3}\,\Omega$ m.[24] With $\mu_0 = 4\pi \times 10^{-7}$ V s/A m and $\omega = 2\pi \times 9.47$ GHz, this yields a minimum penetration depth of $2.45\times 10^{-4}$ m which is $\sim$5 times higher than the disk thickness. Moreover, our measurements on similar polycrystalline $FeCr_2S_4$ samples show that the integral intensity of the ESR signal is essentially the same as in single crystals. In the case of a skin effect this cannot be expected because of the considerably higher ratio of surface to volume for polycrystals as compared to single crystals.

These facts indicate that the skin effect does not influence our results.

Finally, it is necessary to note that the observed peculiarities of the ESR spectra below 125 K point to considerable microscopic magnetic changes, and correlate well with the dc magnetization and ac susceptibility data,[7,8] which show strong variations of the macroscopic magnetic properties in this temperature range. Further studies are necessary to clarify the origin of these transformations.

## V. CONCLUSION

We have investigated the electron-spin resonance of single crystals of a $FeCr_2S_4$ ferrimagnetic semiconductor. We observed large temperature variations of the resonance fields due to the magnetocrystalline anisotropy. For the easy magnetization direction (100) the anisotropy field causes a strong decrease of the resonance field with decreasing temperature. Below 60 K the resonance in this direction is suppressed. For the hard magnetization directions (110) and (111) the anisotropy field considerably shifts the resonance to higher fields. In these hard magnetization directions additional low-field resonance lines at temperatures below 125 K were observed. A nonmonotonic temperature behavior of the integral intensity and of the resonance linewidth of the main resonance lines was found, which indicates substantial changes of the magnetic relaxation processes in the studied compound below 125 and 60 K.


[1] A. P. Ramirez, R. J. Cava, and J. Krajewski, Nature (London) **386**, 156 (1997).

[2] M. S. Park, S. K. Kwon, S. J. Youn, and B. I. Min, Phys. Rev. B **59**, 10 018 (1999).

[3] R. P. van Stapele, in *Ferromagnetic Materials*, edited by E. P. Wohlfarth (North-Holland Publishing Co., Amsterdam, 1982), Vol. 3, p. 603.

[4] R. P. van Stapele, J. S. van Wieringen, and P. F. Bongers, J. Phys. (Paris), Colloq. **32**, C1-53 (1971).

[5] L. Goldstein, P. Gibart, and L. Brossard, in *Magnetism and Magnetic Materials*. 21th Annual Conference, Philadelphia, edited by J. J. Becker, G. H. Lander, and J. J. Rhyne, AIP Conf. Proc. No. 29 (AIP, New York, 1976), p. 405.

[6] V. Tsurkan, D. Samusi, V. Pop, E. Burzo, M. Neumann, M. Demeter, M. Baran, R. Szymczak, and H. Szymczak, in *Interface Controlled Materials*, edited by M. Rühle and H. Gleiter, Proc. Europ. Congr. on Advanced Materials and Processes (EUROMAT 99), Munchen, Germany, 1999 (WILEY-VCH Verlag, Weinheim, 2000), Vol. 9, p. 50.

[7] V. Tsurkan, M. Baran, R. Szymczak, H. Szymczak, and R. Tidecks, Physica B **296**, No. 4 (2001).

[8] V. Tsurkan, J. Hemberger, S. Klimm, M. Klemm, A. Loidl, S. Horn, and R. Tidecks, J. Phys.: Condens. Matter (to be published).

[9] H. Schäfer, *Chemische Transportreaktionen* (Verlag Chemie, Weinheim, 1962).

[10] A. G. Gurevich and G. A. Melkov, *Magnetization Oscillations and Waves* (CRC Press, Boca Raton, FL, 1996), Chap. 2.

[11] C. Kittel, Phys. Rev. **73**, 155 (1948).

[12] C. Kittel, Phys. Rev. **76**, 743 (1949).

[13] E. Schlömann, in *Solid State Physics in Electronics and Telecommunication* (Academic Press, New York, 1960), Vol. 3, p. 322.

[14] S. B. Berger and H. L. Pinch, J. Appl. Phys. **38**, 949 (1967).

[15] S. A. Altschuler and B. M. Kozyrev, *Electron Paramagnetic Resonance in Transition Element Compounds* (Nauka, Moscow, 1972), p. 428.

[16] S. Krupicka, *Physik der Ferrite und der verwandten Magnetischen Oxide* (Academia Verlag der Tsechoslovakischen Academie der Wissenschaften, Prag, 1973), Chap. 5.

[17] G. R. Hoy and K. P. Singh, Phys. Rev. **172**, 514 (1968).

[18] M. R. Spender and A. H. Morrish, Solid State Commun. **11**, 1417 (1972).

[19] A. M. van Diepen and R. P. van Stapele, Solid State Commun. **13**, 1651 (1973).

[20] F. K. Lotgering, A. M. van Diepen, and J. F. Olijhoek, Solid State Commun. **17**, 1149 (1975).

[21] L. F. Feiner, J. Phys. C **15**, 1515 (1982).

[22] H. Göbel, J. Magn. Magn. Mater. **3**, 143 (1976).

[23] J. D. Jackson, *Classical Electrodynamics* (Wiley, New York, 1975), p. 298.

[24] V. Tsurkan, I. Fita, M. Baron, R. Puzniak, D. Samusi, R. Szymczak, H. Szymczak, S. Klimm, M. Klemm, S. Horn, and R. Tidecks, J. Apl. Phys. (to be published).